Translational Oncology 26 (2022) 101547

Contents lists available at ScienceDirect

Translational Oncology

journal homepage: www.elsevier.com/locate/tranon

# Development and validation of a microenvironment-related prognostic model for hepatocellular carcinoma patients based on histone deacetylase family

Linxin Teng [a,d,1], Zhengjun Li [b,d,1], Yipeng Shi [a], Zihan Gao [a], Yang Yang [a], Yunshan Wang [c], Lei Bi [a,d,*]

[a] School of Integrated Chinese and Western Medicine, Nanjing University of Chinese Medicine, 138 Xianlin Road, Nanjing, Jiangsu 210023, China
[b] College of Health Economics Management, Nanjing University of Chinese Medicine, 138 Xianlin Road, Nanjing, Jiangsu 210023, China
[c] Department of Clinical Laboratory, The Second Hospital, Cheeloo College of Medicine, Shandong University, 247 Beiyuan Street, Jinan, Shandong 250033, China
[d] Jiangsu Provincial Engineering Research Center of TCM External Medication Development and Application, Nanjing 210023, China

ARTICLE INFO

*Keywords:*
Histone deacetylase
Tumor microenvironment
Fatty acid metabolism
Hepatocellular carcinoma
Macrophages

ABSTRACT

*Background:* Histone deacetylase (HDAC) family can remove acetyl groups from histone lysine residues, and their high expression is closely related to the poor prognosis of hepatocellular carcinoma (HCC) patients. Recently, it has been reported to play an immunosuppressive role in the microenvironment, but little is known about the mechanism.

*Methods:* Through machine learning, we trained and verified the prognostic model composed of HDACs. CIBERSORT was used to calculate the percentage of immune cells in the microenvironment. Based on co-expression network, potential targets of HDACs were screened. After that, qRT-PCR was employed to evaluate the expression of downstream genes of HDACs, while HPLC-CAD analysis was applied to detect the concentration of arachidonic acid (AA). Finally, Flow cytometry, WB and IHC experiments were used to detect CD86 expression in RAW246.7.

*Results:* We constructed a great prognostic model composed of HDAC1 and HDAC11 that was significantly associated with overall survival. These HDACs were related to the abundance of macrophages, which might be attributed to their regulation of fatty-acid-metabolism related genes. In *vitro* experiments, the mRNA expression of ACSM2A, ADH1B, CYP2C8, CYP4F2 and SLC27A5 in HCC-LM3 was significantly down-regulated, and specific inhibitors of HDAC1 and HDAC11 significantly promoted the expression of these genes. HDAC inhibitors can promote the metabolism of AA, which may relieve the effect of AA on the polarization of M1 macrophages.

*Conclusions:* Our study revealed the blocking effect of HDAC1 and HDAC11 on the polarization of macrophages M1 in the microenvironment by inhibiting fatty acid metabolism.

## Introduction

Histone deacetylase (HDAC) family is a group of enzymes that control the balanced acetylation of lysines in the tails of the core histones, which is one of the most extensively studied epigenetic modifications. There are 18 HDACs identified to date, which can be divided into four classes based on their homology to the respective yeast orthologues [1,2]. Classes I (HDAC1, 2, 3, and 8), II (HDAC4, 5, 6, 7, 9 and 10) and IV (HDAC11) are $Zn^{2+}$-dependent enzymes, while Class III (SIRT1-7) is $NAD^{+}$-dependent [2,3]. Unlike class I HDACs (usually present in the nucleus), classes II, III and IV HDACs tend to shuttle between the nucleus and cytoplasm [1]. High expression of HDACs was found in hepatocellular carcinoma (HCC) patients and was significantly associated with poor prognosis [4–6]. It has been reported that the expression of HDACs could reduce the sensitivity of sorafenib [6] and was closely related to metabolic reprogramming and immune response [7–9], making them attractive targets in cancer research.

With the deepening of investigation, the role of HDACs in HCC has been highlighted. Silencing HDAC2 could significantly block the PPARγ signaling pathway, thereby reducing fat synthesis and treating HCC

* Corresponding author at: School of Integrated Chinese and Western Medicine, Nanjing University of Chinese Medicine, 138 Xianlin Road, Jiangsu 210023, China.
*E-mail address:* lbi@njucm.edu.cn (L. Bi).
[1] These authors contributed equally to this work.

https://doi.org/10.1016/j.tranon.2022.101547
Received 9 March 2022; Received in revised form 25 May 2022; Accepted 26 September 2022

[10]. In addition, our previous research suggested that the loss of HDAC11 could inhibit glycolysis and tumor growth, which was attributed to its activation of LKB1 / AMPK pathway [9]. Despite promising preclinical results, the clinical studies of HDAC inhibitors (HDACi) in patients with solid tumors had furnished disappointing outcomes [11]. The intrinsic or acquired drug resistance of single HDACi may be due to cross talk and compensation among HDACs [12], therefore further study of HDACs would bring to fruition that the therapeutic potential of HDACi. All in all, HDACs play an important role in HCC therapy, and the way HDACs work is urgently required.

HDACs have been widely reported to play an important role in immunity. They were found to drive the increase of regulatory T cell (Treg) levels in myeloid leukemia patients [13]. Furthermore, acetylation of Forkhead Box P3 (FOXP3) mediated by class II HDACs, especially HDAC9, helped to enhance Treg function and prevented the development of colitis [14,15]. HDAC1, HDAC3 and HDAC11 could reduce expression of IFN-γ, indicating that the loss of IFN-γ was an important approach for HDACs to take effect [16]. It is worth mentioning that class IIa HDACs can inhibit the differentiation of macrophages, which may also be related to its regulation of IFN-γ [17]. T cells are one of the main sources of IFN-γ, and the chromatin reprogramming of $CD4^+$ T cells by HDACi could reverse its inactivation [18]. Moreover, inhibition of HDAC6 expression was beneficial to the proliferation and activation of T cells in the microenvironment [19]. In conclusion, HDACs could promote tumor development by inhibiting the immune response, but its mechanism still needs to be further studied. The aim of this study is to explore the role of HDACs in microenvironment, so as to provide a new perspective for their application in the treatment of HCC.

## Materials and methods

### *Data acquisition*

In this study, we downloaded **the gene expression profiles** of 357 tumor tissues and 49 normal tissues from TCGA (https://cancergenome.nih.gov/) database. Then, we employed the hold-out method to divide HCC samples into the Training Set and the Validation Set (7:3). Non-TCGA cohort data were acquired from ICGC (https://daco.icgc.org/), Gene Expression Omnibus (GEO) (https://www.ncbi.nlm.nih.gov/geo/) and ArrayExpress (https://www.ebi.ac.uk/arrayexpress/) databases and were used as test sets (test cohort one: 260 HCC tissues from ICGC; test cohort two: 221 HCC tissues from GSE14520 [20], test cohort three: 39 HCC tissues from ArrayExpress). The clinical information of patients in these datasets was shown in Table. S1. In addition, we obtained the GSE109211 [21] from GEO database to explore the effect of HDACs on sorafenib.

### *Differential expression gene analysis*

Before the differential expression gene (DEG) analysis, we first standardized the sequencing data by log2(TPM + 1). Then, the "limma" package of R software (version 3.6.1, https://www.r-project.org) was used to calculate the difference of gene expression between tumor and normal tissues, and HDACs with false discovery rate (FDR) less than 0.05 were considered to have significant changes.

### *Survival analysis and multivariate Cox regression analysis*

Based on the Kaplan-Meier (KM) algorithm, HDACs that significantly ($p < 0.1$) affected OS from the training set ($n = 250$) were identified. Then, we employed least absolute shrinkage and selection operator (LASSO) Cox regression analysis to select these HDACs, which were independent prognostic factors for HCC patients. The "survival" package was used to screen the variables that accorded with the proportional hazards (PH) assumption. Finally, in order to solve the problem of multicollinearity in the model, the correlation coefficient between variables and the square root of variance inflation factor (VIF) were required to be less than 0.5 and 2 respectively.

### *Evaluation of multivariate Cox regression model*

The risk score was calculated by the following formula: risk score $= \sum_{i=1}^{n}(Coef_i + Expr_i)$ ($Coef_i$ was Cox regression coefficients and $Expr_i$ was gene expression value). We evaluated the model with time-dependent Receiver Operating Characteristic (ROC) curve in the validation set ($n = 107$) and tested the model in three non-TCGA sets ($n =$ 260 / 221 / 39).

### *Construction and validation of prognostic nomogram*

Forward selection method was utilized for further integrating the clinical information into the multivariate Cox regression model and constructing the prognostic nomogram. Moreover, the calibration plot and ROC curve were used to evaluate the efficiency of nomogram.

### *Evaluation of immune score and immune cell type*

"CIBERSORT" and "xCell" were mainly employed to calculate the percentages of immune cells. Unlike the Nonnegative Matrix Factorization (NMF) algorithm used by CIBERSORT, xCell was based on deconvolution.

### *Enrichment analysis and Gene Set Variation Analysis*

FDR < 0.05 was considered as the cut-off criterion of the result of Gene Set Enrichment Analysis (GSEA). As for Gene Ontology (GO) and Kyoto Encyclopedia of Genome and Genome (KEGG) enrichment analyses, we would prefer to screen results that were significantly enriched according to $p < 0.05$. We also performed Gene Set Variation Analysis (GSVA) derived from risk score. After that, the "limma" package was further used to identify the KEGG pathways with significant differences ($|\log2FC| > 0.3$ & FDR < 0.05).

### *Establishment of co-expression network of HDACs*

The genes that were highly negatively correlated ($r < -0.5$ & $p < 0.05$) with the expression of HADCs and significantly down-regulated in HCC patients (log2FC < -1 & FDR < 0.05) were speculated to be regulated by HDACs. Then, the mutation information of these genes was obtained from cBioPortal (https://www.cbioportal.org/) and 380 HCC samples were brought into this study. And the results of immunohistochemistry from The Human Protein Atlas (https://www.proteinatlas.org/) database **were employed** to verify the changes in protein expression. Finally, we established a co-expression network of HDACs through Cytoscape (version 3.6.0, https://cytoscape.org) based on previous results.

### *Cell lines and cell culture*

The human normal liver cell line (HL-7702), human hepatoma cell lines (BEL-7402, HepaRG and SMMC-7721) and RAW246.7 were obtained from the Shanghai Institute of Biochemistry and Cell Biology. Human liver cancer cell lines (HCC-LM3, HepaRG and HuH-7) were purchased from Jiangsu Key GEN Bio TECH Corp. All these cell lines were cultured in DMEM medium supplemented with 10% FBS and 1% PS and maintained in a humid atmosphere with 5% CO2 at 37°C.

### *Quantitative Real-Time PCR (qRT-PCR)*

The primer sequences used in the qRT-PCR reaction were shown in Table. S2. Total RNA was extracted from HL-7702 and liver cancer cell

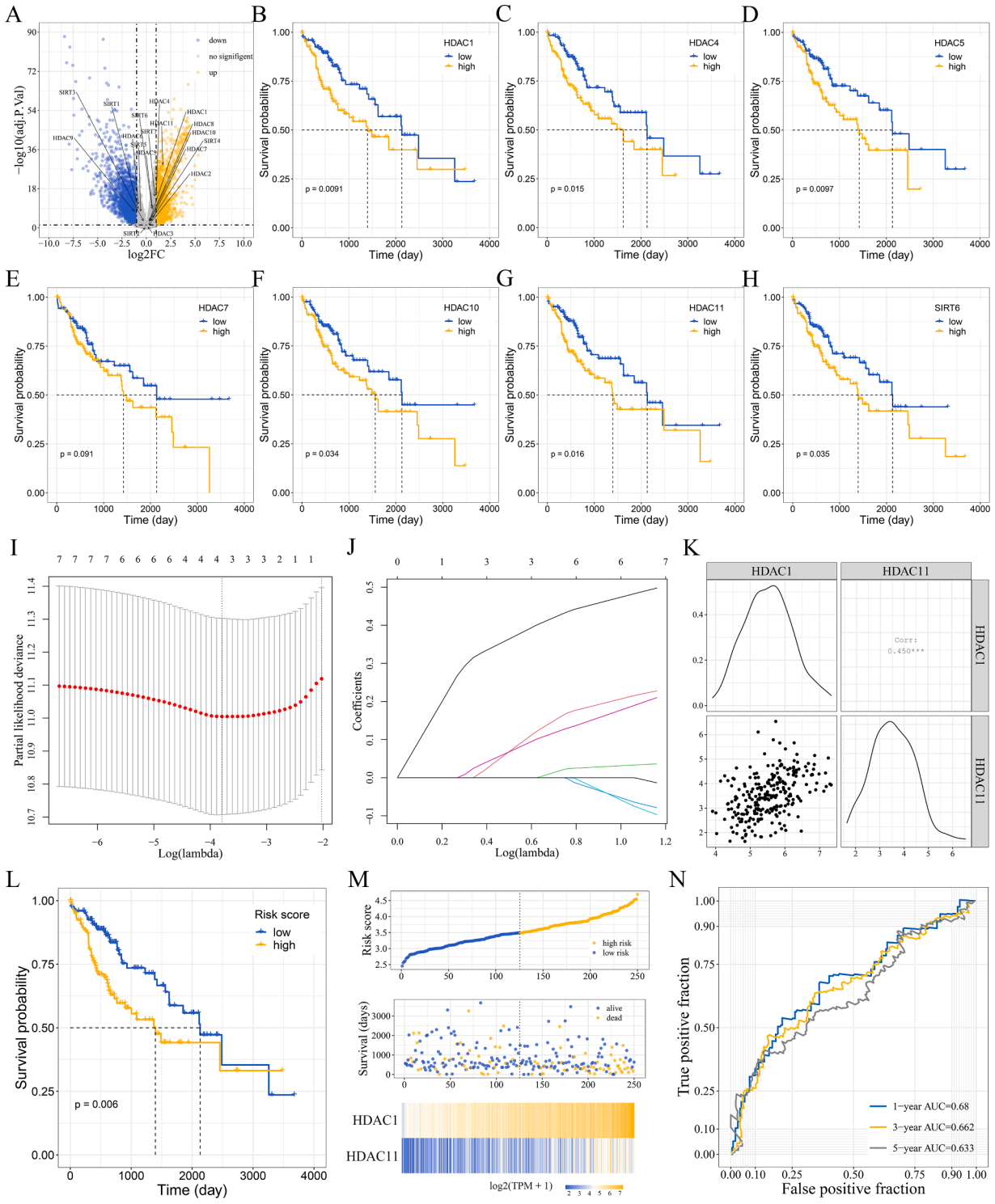


**Fig. 1.** The result of Cox regression analysis of HCC patients in training set. **A.** DEG analyses of HDACs. **B-H.** Survival analyses of HDAC1, HDAC4, HDAC5, HDAC7, HDAC10, HDAC11 and SIRT6. **I, J.** LASSO Cox regression analyses of HDACs. **K.** Correlation analysis of HDAC1 and HDAC11. **L, M.** Survival analysis of Cox regression model. **N.** Time-dependent ROC analyses of Cox regression model at 1-, 3- and 5-year.

lines with RNAiso plus reagent. Then, cDNA was converted from the total RNA and was further used for amplification in the qRT-PCR system (Applied Biosystems, Foster City, CA, USA) with SYBR Green and primers. Finally, the $2^{-\Delta\Delta Ct}$ method was employed to calculate the result. Two inhibitors were used in the experiment. Pyroxamide (specific HDAC1 inhibitor) [22] was **obtained** from MedMol (Shanghai, China), while garcionl (specific HDAC11 inhibitor) [23] was bought from GlpBio (California, USA).

*HPLC-CAD analysis*

HCC cells were treated with HDAC inhibitors for 24 h and then incubated with culture medium containing Arachidonic acid (AA, 0.5mM), which was purchased from Solarbio (Beijing, China). After 24 hours, the cell supernatant was collected and added with equal volume of methanol. The samples were centrifuged and filtered before being tested in the machine. HPLC-CAD analysis was performed on a Dionex

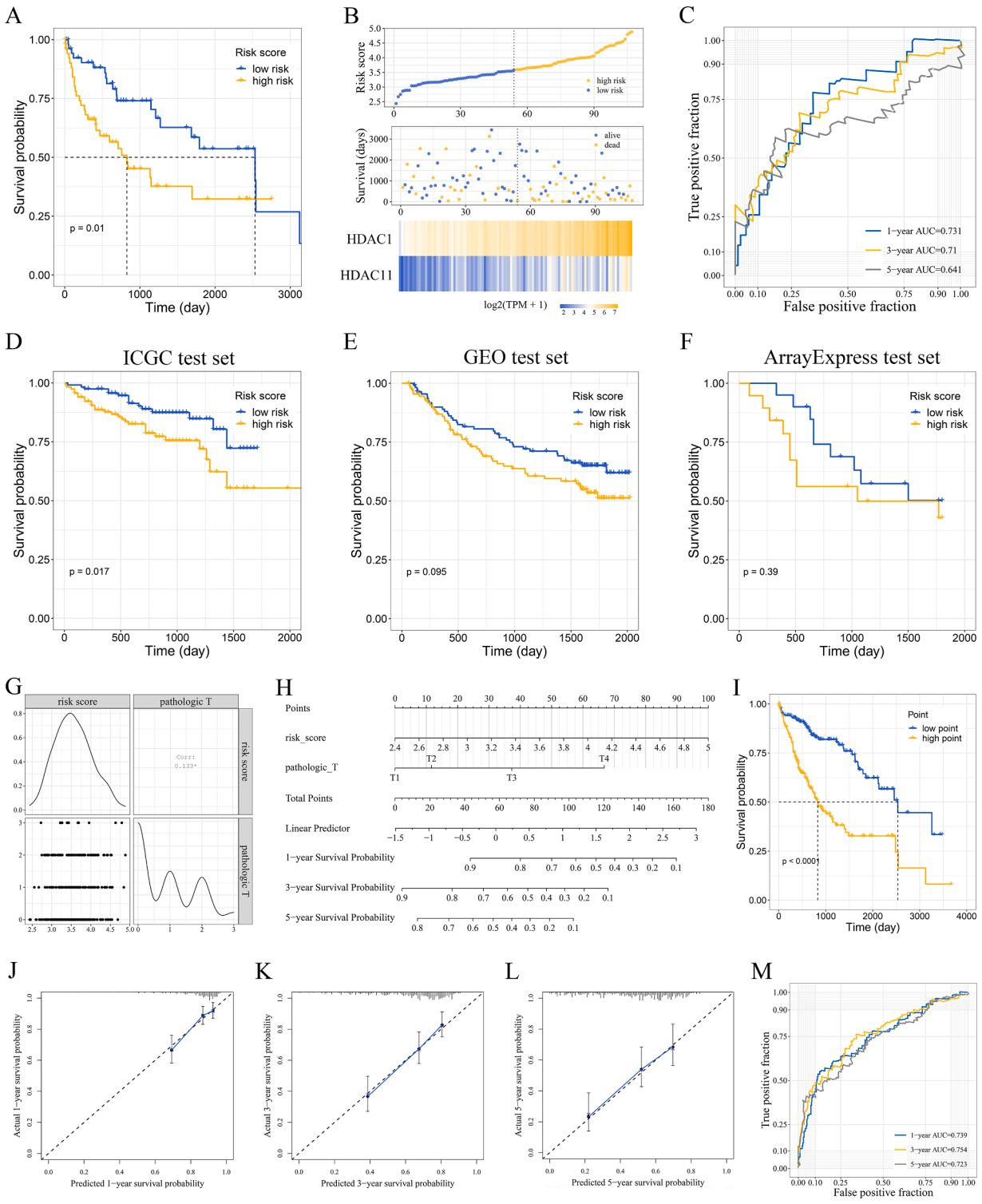


**Fig. 2.** The result of Cox regression analyses of HCC patients in the validation set and test sets. **A, B.** Survival analysis of Cox regression model in the validation set. **C.** Time-dependent ROC analyses of Cox regression model at 1-, 3- and 5-year in validation set. **D-F.** Survival analyses of Cox regression model in ICGC, GEO and ArrayExpress test sets. **G.** Correlation analysis of risk score and pathologic T-stage in TCGA dataset. **H.** The nomogram for OS in TCGA dataset. **I.** Survival analysis of nomogram model in TCGA dataset. **J-L.** Calibration plots of nomogram model at 1-, 3- and 5-year. **M.** Time-dependent ROC analyses of nomogram model at 1-, 3- and 5-year.

UltiMate 3000 HPLC (Thermo Fisher Scientific, USA) with the mobile phase consisting of pure water (A) – methanol (B) at a flow rate of 0.5 mL / min (0 ~ 5 min, 50% B; 5 ~ 10 min, 70% B; 10 ~ 15 min, 85% B; 15 ~ 20 min, 85% B; 20 ~ 30 min, 50% B). A Dionex Acclaim 120 $C_{18}$ column (4.6 × 250 mm, 5 μm) was used for the chromatographic separation at 37°C. The conditions of the CAD detector were as follows: sampling frequency 10 Hz, filer constant 5.0 s and power rate 1.00. Finally, the concentration of AA in each sample was calculated according to the standard curve.

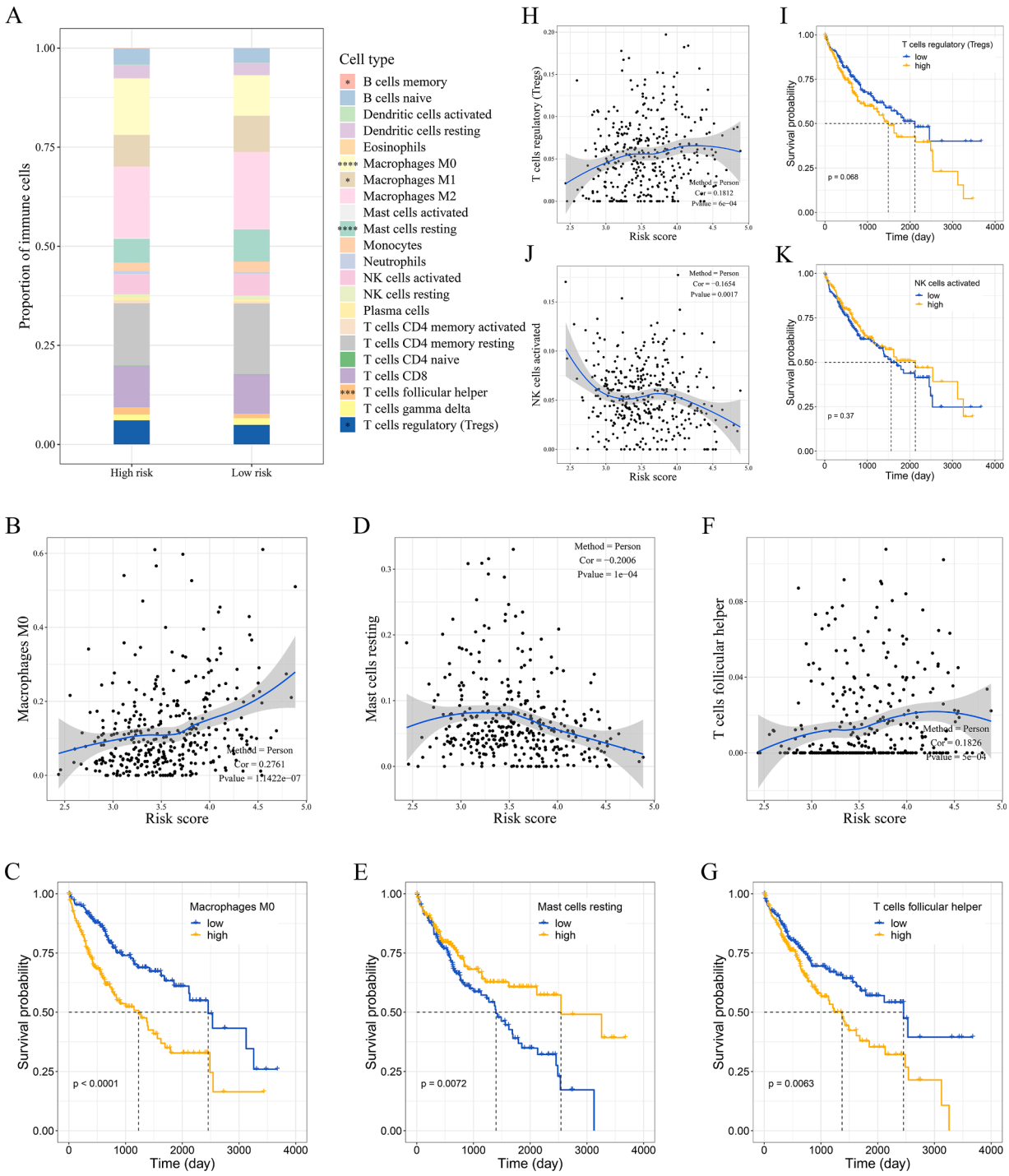


**Fig. 3.** Evaluation of immune cells in high-risk and low-risk groups of HCC patients in TCGA dataset. **A.** Proportion of immune cells in high-risk and low-risk groups. **B.** Correlation analysis of "macrophages M0" and risk score. **C.** Survival analysis of "macrophages M0". **D.** Correlation analysis of "mast cells resting" and risk score. **E.** Survival analysis of "mast cells resting". **F.** Correlation analysis of "T follicular helper cells" and risk score. **G.** Survival analysis of "T follicular helper cells". **H.** Correlation analysis of "T cells regulatory" and risk score. **I.** Survival analysis of "T cells regulatory". **J.** Correlation analysis of "NK cells activated" and risk score. **K.** Survival analysis of "NK cells activated".

*Flow cytometry*

RAW246.7 were placed into a 24-well plate and cultured under standard conditions for one day. LPS (Beyotime, Shanghai, China) and different concentrations of AA were added into the supernatant. After 24 hours, the digested cells were resuspended with precooled PBS (containing 1% BSA). Then, the cells were incubated with PE-labeled CD86 (Elabscience, Wuhan, China) at 4°C for 30 min. Thereafter, the samples were washed with PBS and resuspended for detection by flow cytometry.

*Western blot*

The treated-RAW246.7 cells were extracted on ice with RIPA lysis buffer containing PMSF and protease inhibitor. According to the standard curve, the protein concentrations of the samples were measured with BCA protein assay kit. The protein samples were isolated by SDS-

PAGE and then transferred to PVDF membrane. After sealing, the PVDF membranes were incubated with the primary antibody against CD86 (ABclonal, Wuhan, China) overnight, which was diluted according to 1:1000. Then, the membranes were washed with TBST for 3 times and incubated with secondary antibody (1:8000) at room temperature for 1 hour. Finally, the film was cleaned again with TBST and imaged with ECL. The result was analyzed by Image J software according to optical density (OD) value.

### *Immunohistochemistry staining (IHC)*

As shown in Fig. S1, cell co-culture was carried out in 24-well plates. IHC staining was performed using cell climbing sheets obtained from co-culture. The cells were fixed (4% paraformaldehyde), permeabilized (0.3% Triton X-100), peroxidase eliminated (3% hydrogen peroxide) and sealed (5% BSA) in turn. After that, the samples were placed in the primary antibody against CD86 (1:200) overnight and then incubated with the secondary antibody purchased from Absin (Shanghai, China). Finally, the antibody was developed with DAB kit from Solarbio (Beijing, China) and the result was evaluated by Image J software according to mean density (mean density $= \frac{IOD}{Area}$).

### *Statistical analysis*

Statistical analysis was performed using R and GraphPad Prism 8.0 software. Student's t-test test and one-way analysis of variance (ANOVA) were used when variance was homogeneous, while Wilcoxon rank sum test was used when variance was not homogeneous. A $p$-value $< 0.05$ was considered a significant difference.

## Results

### *Prognostic-related HDACs in HCC*

We found 15 of 18 HDACs (except HDAC2, HDAC3 and SIRT2) that were significantly differentially expressed between tumor tissues and normal tissues by DEG analysis (Fig. 1A). As shown in Fig. 1B-H, seven HDACs (HDAC1, HDAC4, HDAC5, HDAC7, HDAC10, HDAC11 and SIRT6) were significantly associated with the prognosis of patients. High expression of all seven HDACs was accompanied by short overall survival (OS), which suggested that these HDACs might play a role in promoting the development of HCC.

### *HDAC1 and HDAC11 synergistically promote HCC progression*

The result of LASSO Cox regression analysis was shown in Fig. 1I-J, HDAC1, HADC4, HADC5 and HDAC11 were considered to be characteristic variables. HDAC4 did not fit the PH hypothesis, while HDAC5 was highly correlated with HDAC1 (correlation coefficient $> 0.5$). As a result, they were removed from the model. As shown in Fig. 1K, HDAC1 and HDAC11 were finally included in the model and the formula of risk score was as follows: risk score = 0.524 * expression of HDAC1 + 0.177 * expression of HDAC11. The coefficients of these two HDACs in the model were both positive numbers, suggesting a possible synergistic role of HDAC1 and HDAC11 in promoting HCC. As expected, the risk score was significantly ($p = 0.006$) correlated with the prognosis of HCC (Fig. 1L-M). In addition, the area under curve (AUC) values of 1-, 3- and 5-year were 0.680, 0.662 and 0.633, respectively (Fig. 1N), which indicated that risk score could be used to predict the survival status of HCC patients.

The performance of the model on the validation set showed basically the same result (Fig. 2A-B). The AUC values of 1-, 3- and 5-year were 0.731, 0.710 and 0.641, respectively (Fig. 2C). In addition, we further tested the model in HCC patients from different regions (Japan, the United States and France). As shown in Fig. 2D-F, risk score was significantly ($p = 0.017$) associated with the OS of HCC patients in test set one (Japan cohort), while the OS of patients in test set two (the United States cohort) and test set three (France cohort) were not significant ($p = 0.095$ and $p = 0.39$). This unexpected result could be attributed to the differences in data measurement and standardization between microarray and RNA-seq. HDAC1 and HDAC11 were not identified as independent prognostic features in test set two and test set three (Fig. S2), and the proportion of sorafenib responders in low-risk group was much higher than that in high-risk group (Fig. S3), implying the synergistic role of these two HDACs in HCC progression.

### *Risk score and pathologic T are independent prognostic factors in nomogram*

First, univariate Cox regression analyses were performed on eleven clinical factors to screen for meaningful independent prognostic factors. As shown in Table. S3, three factors including pathologic M ($p = 0.020$), pathologic T ($p = 1.954e-08$) and pathologic stage ($p = 8.364e-07$) were found significantly associated with OS. Then, risk score and pathologic T were brought into the nomogram by forward selection, and multicollinearity among variables was excluded (Fig. 2G-H). Through the survival analysis (Fig. 2I), we found that the point of **nomogram** had a more significant ($p = 4.224e-09$) impact on the prognosis of patients **compared with the risk score**. Moreover, calibration plots and time-dependent ROC curves (1-, 3- and 5-year correspond to 0.739, 0.754 and 0.723 respectively) also showed a good predictive accuracy of the nomogram points (Fig. 2J-M), indicating potential clinical application of the risk score calculated from HDACs.

### *Immune cells affected by the expression of HDAC1 and HDAC11*

Research showed that HDAC1 and HDAC11 were related to the infiltration of many kinds of immune cells. They could facilitate the polarization of Treg and block the secretion of IFN-γ [16,24]. To investigate whether HDAC1 and HDAC11 could jointly promote HCC by regulating anti-tumor immune response, we tried to explore the immune cells implicated with them. As shown in Fig. 3A, the proportions of six kinds of immune cells were significantly different between high-risk group and low-risk group. Compared with the high-risk group, the ratios of "macrophages M1" ($p = 0.011$) and "mast cells resting" ($p = 9.415e-04$) in the low-risk group were **significantly reduced**, while the ratios of "B cells memory" ($p = 0.014$), "T follicular helper (TFH) cells" ($p = 0.004$), "T cells regulatory" ($p = 0.011$) and "macrophages M0" ($p = 8.768e-04$) were **significantly increased**. Among the 22 types of immune cells, "macrophages M0" had the highest correlation coefficient ($r = 0.276$) with risk score, and was closely related to poor prognosis (Fig. 3B-C). The correlation coefficient between "mast cells resting" and risk score was -0.201, and a high proportion of "mast cells resting" indicated a good prognosis (Fig. 3D-E). The third highest correlation coefficient with risk score was "T cells follicular helper" ($r = 0.183$), which might be negatively correlated with OS (Fig. 3F-G). Although there was a correlation between "T cells regulatory" and risk score ($r = 0.181$), the effect of "T cells regulatory" on OS was not significant ($p = 0.068$, Fig. 3H-I). **Different from** "T cells regulatory", "NK cells activated" and risk score were negatively correlated ($r = -0.165$, Fig. 3J). As shown in Fig. 3K, patients with high levels of "NK cells activated" had a poor prognosis, **but there was no significant difference in OS between the two groups** ($p = 0.37$). In conclusion, HDAC1 and HDAC11 might play an immunosuppressive role by affecting the abundance of immune cells, resulting in a poor prognosis for HCC patients.

### *Immune-related pathways regulated by HDAC1 and HDAC11*

To further understand the mechanism of anti-tumor immunity regulated by HDACs in HCC, we performed GSVA analysis to identify the pathways affected by HDAC1 and HDAC11 expression. Low-risk group

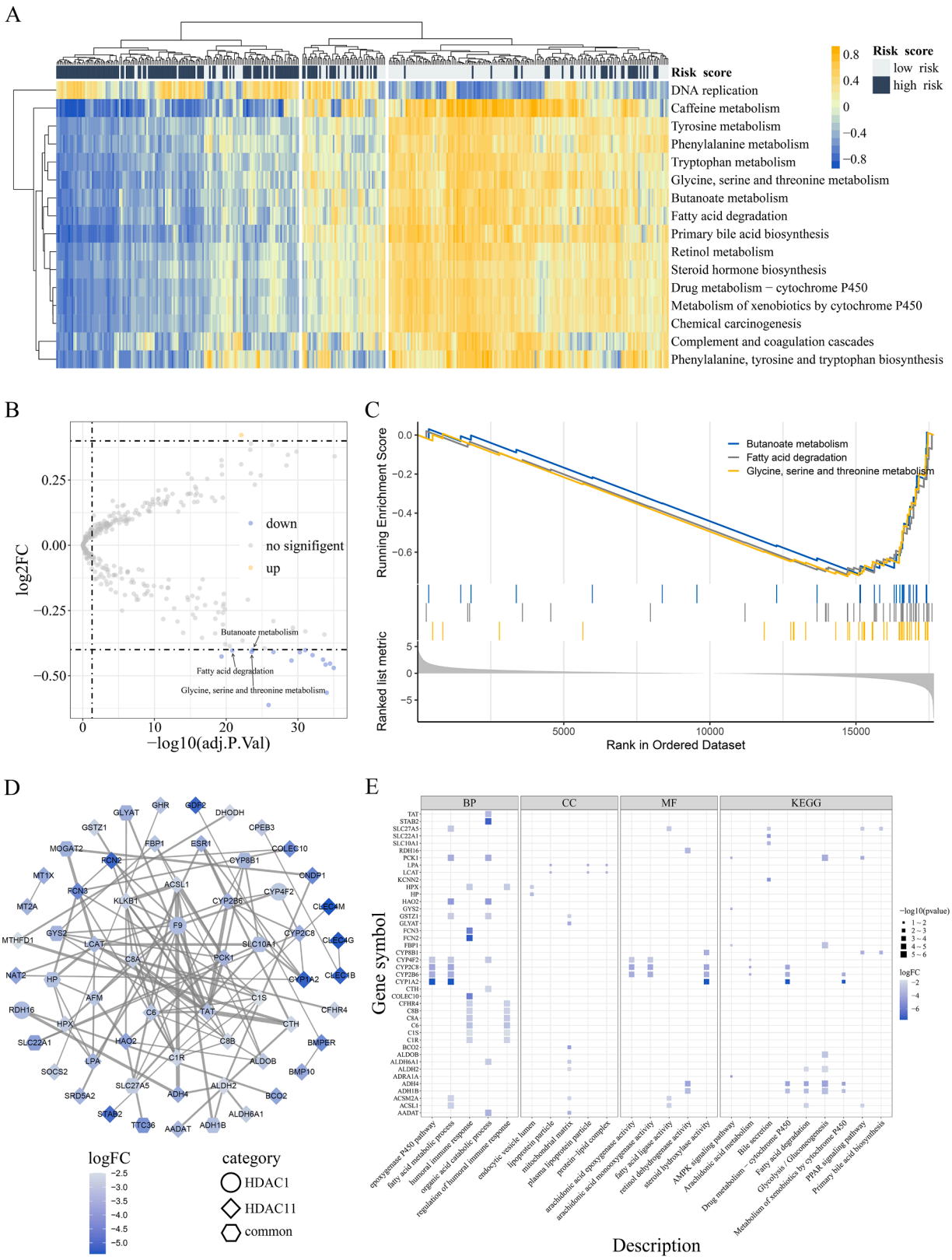


**Fig. 4.** The result of GSVA of high-risk and low-risk groups and enrichment analysis of co-expression network. **A.** The ES of KEGG pathway in high-risk group and low-risk group. **B.** Differential pathway analysis between high-risk group and low-risk group. **C.** GSEA of HCC patients. **D.** Co-expression network of HDAC1 and HDAC11. **E.** Enrichment analysis of co-expression network.

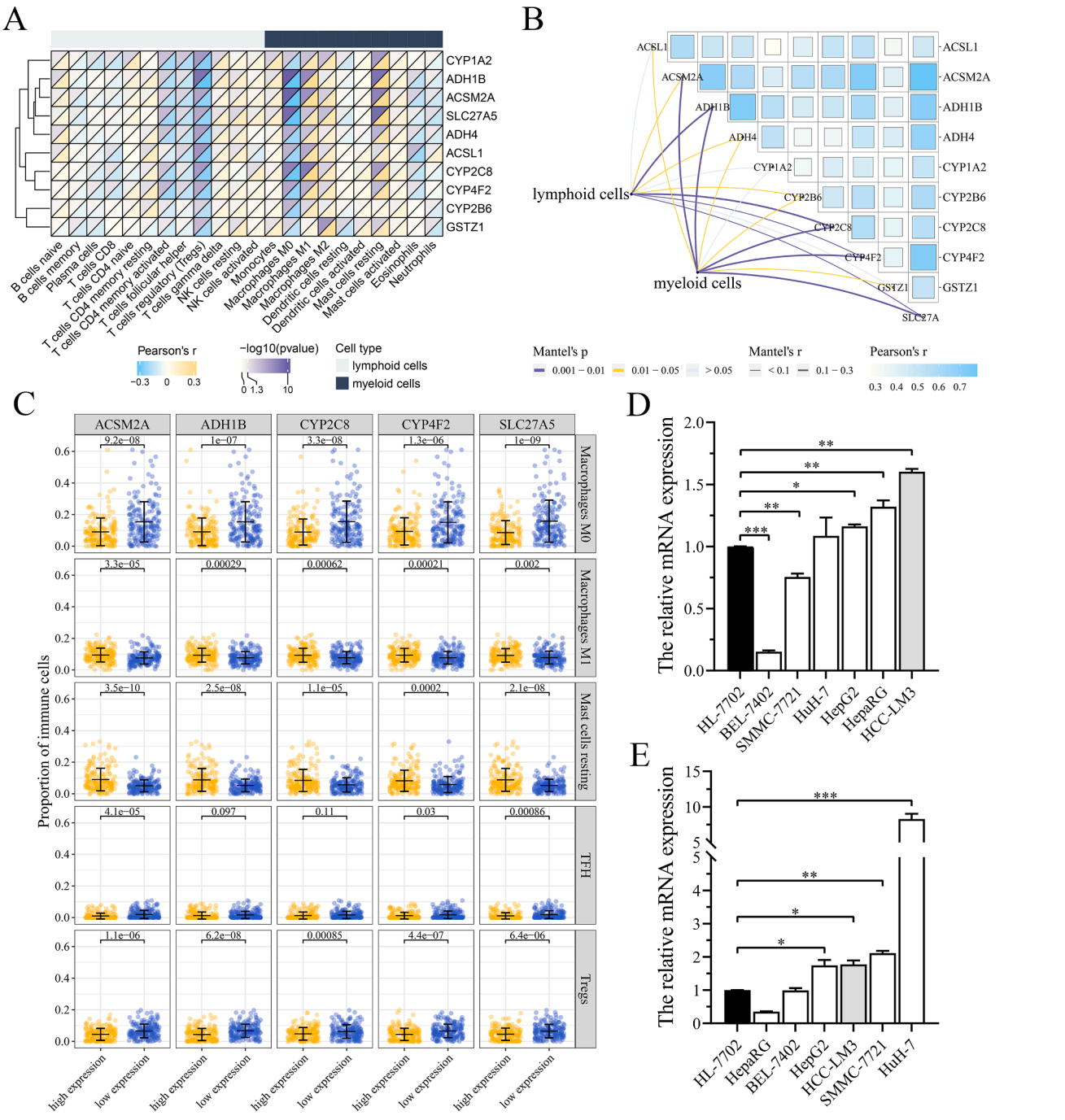


*(caption on next page)*

**Fig. 5.** HDACs can inhibit the expression of fatty acid metabolism related genes, which is significantly associated with the level of immune cells. **A.** Correlation analysis of **fatty acid** metabolism related genes and immune cells. **B.** Mantel test of **fatty acid** metabolism related genes and lymphoid cells and myeloid cells. **C.** T test of the proportion of "Macrophages M0", "Mast cells resting", "T follicular helper cells" and "T cells regulatory" in high- and low-expression groups of fatty acid metabolism related genes. **D.** The expression of HDAC1 in normal liver and HCC cell lines ($n = 3$). **E.** The expression of HDAC11 in normal liver and HCC cell lines ($n = 3$). **F.** The expression of ACSM2A, ADH1B, CYP2C8, CYP4F2 and SLC27A5 in HCC-LM3 ($n = 3$). **G.** The expression of ACSM2A, ADH1B, CYP2C8, CYP4F2 and SLC27A5 in HCC-LM3 after treatment with pyroxamide and garcionl ($n = 3$). *: $p < 0.05$, **: $p < 0.01$, ***: $p < 0.001$, ****: $p < 0.0001$.

got higher enrichment scores (ES) than high-risk group in "glycine, serine and threonine metabolism", "fatty acid degradation" and "butanoate metabolism" related pathways (Fig. 4A). These three pathways were included in the 38 pathways with significant differences between high-risk and low-risk groups (Fig. 4B and Table. S4). The result of GSEA analysis of DEGs in tumor tissues compared with normal tissues also showed that the three pathways were enriched at the bottom, indicating that normal tissues were better than tumor tissues in metabolizing fatty acid and butanoate (Fig. 4C). As the essential regulatory effects of non-essential amino acids (glycine and serine), fatty acid and butanoate have been reported on tumor immunity [25–27], so we speculated that HDAC1 and HDAC11 might inhibit immune response by affecting the metabolism of these metabolites.

### *Co-expression network of HDAC1 and HDAC11*

In order to predict the genes regulated by HDACs, a co-expression network was established. Firstly, we preliminarily screened out 86 genes that might be inhibited by HDAC1 and HDAC11. The top five genes negatively correlated with **these HDACs** were HP, GYS2, SLC10A1, SLC27A5, and CYPB1 (Fig. S4). As shown in Table. S5, all 86 genes were down-regulated in high-risk group (78 genes with significant differences). What's more, the average mutation frequency of 86 genes was 0.37% (Fig. S5), suggesting these genes might be affected by epigenetics. Accordingly, co-expression network of HDAC1 and HDAC11 was established as shown in Fig. 4D, and the five genes (F9, C8A, C6, TAT and PCK1) located in the center of the network were the key nodes. The enrichment analysis showed that three biochemical reactions related to fatty acid were significantly enriched (Fig. 4E). A total of 11 genes were involved in fatty-acid-metabolism, including ACSL1, ACSM2A, ADH1B, ADH4, ALDH2, CYP1A2, CYP2B6, CYP2C8, CYP4F2, GSTZ1 and SLC27A5. Furthermore, immunohistochemical results showed that, except for ALDH2, ten fatty-acid-metabolism related proteins were down-regulated in HCC patients (Fig. S6). Therefore, the fatty-acid-metabolism related genes might be transcriptionally inhibited by HDAC1 and HDAC11 to play an immunosuppressive role.

### *Immune cells affected by fatty-acid-metabolism related genes*

As shown in Fig. 5A, "Macrophages M0", "TFH" and "Tregs" were negatively correlated with ten fatty-acid-metabolism related genes, while "Macrophages M1" and "Mast cells resting" were positively correlated with these genes. Moreover, we also calculated the proportion of immune cells in ICGC dataset (LIRI-JP), and the result was in line with that in TCGA (Fig. S7). Then, the result of the Mantel test showed that five genes (ACSM2A, ADH1B, CYP2C8, CYP4F2 and SLC27A5) were significantly (Mantel's $r > 0.1$ & $p < 0.05$) correlated with lymphoid cells or myeloid cells (Fig. 5B). As shown in Fig. 5C, the proportion of "Macrophages M0" and "Treg" in the low-expression groups of these five genes increased significantly **($p < 0.05$)**, whereas the ratio of "Macrophages M1" and "Mast cells resting" in the low-expression groups was significantly **($p < 0.05$)** lower than that in the high-expression groups. It has been reported that the high abundance of non-activated macrophages and Tregs are associated with a poor prognosis in HCC patients [21], while macrophages M1 can significantly inhibit tumor growth [28]. Activated mast cells may inhibit the progression of HCC [21], but the relationship between the level of total mast cells and tumor immunity is still unclear. Collectively, fatty-acid-metabolism related genes were regulated by HDAC1 and HDAC11 **might change** the relative abundance of macrophages and Tregs in the tumor microenvironment.

### *The expression of fatty-acid-metabolism related genes is regulated by HDACs*

As shown in Fig. 5D, the expression of HDAC1 in HepG2, HepaRG and HCC-LM3 was significantly **($p < 0.05$)** increased, while its expression in BEL-7402 and SMMC-7721 was significantly **($p < 0.05$)** decreased. As for HDAC11, its endogenous expression of four HCC cell lines (HepG2, HCC-LM3, SMMC-7721 and HuH-7) was significantly **($p < 0.05$)** higher than that of normal liver cell line (Fig. 5E). Unsurprisingly, the expression of ACSM2A, ADH1B, CYP2C8, CYP4F2 and SLC27A5 was decreased significantly **($p < 0.05$)** in HCC-LM3 (Fig. 5F), which had high levels of HDAC1 and HDAC11. Then, specific inhibitors of HDAC1 and HDAC11 were used to further verify their regulatory effects on genes related to fatty-acid-metabolism, and the results were shown in Fig. 5G. Compared with the control group, the expression of these genes was significantly increased in both pyroxamide (HDAC1 inhibitor) and garcionl (HDAC11 inhibitor) groups. Altogether, the results were consistent with bioinformatics predictions, suggesting that HDAC1 and HDAC11 could down regulate the expression of fatty-acid-metabolism related genes.

### *HDAC inhibitors may affect macrophage polarization by promoting arachidonic acid metabolism*

The result of Ingenuity Pathway Analysis (IPA) showed that ACSM2A, ADH1B, CYP2C8, CYP4F2 and SLC27A5 were considered to directly participate in fatty acid metabolism, especially arachidonic acid (Fig. 6A). As shown in Fig. 6B and Fig. S8, the result of HPLC-CAD analysis showed that the AA concentration in garcionl group and combination group was significantly lower than that in the control group, suggesting that HDACs could inhibit the metabolism of AA. In addition, compared with HDAC11 inhibitor group, the content of AA in the combination group was significantly ($p < 0.05$) reduced. The experimental results of flow cytometry (Fig. 6C), WB (Fig. 6D) and IHC (Fig. 6E-F) all contributed to the conclusion that AA (0.5mM) could significantly inhibit RAW246.7 polarization to M1 macrophages. As shown in Fig. 6E-F, the expression of CD86 of RAW246.7 was not affected by HCC-LM3 without HDAC inhibitor treatment in the co-culture system. Further results showed that HCC-LM3 pre-treated with HDAC11 inhibitor significantly increased CD86 expression of RAW246.7. Although there was no significant difference in CD86 expression of RAW246.7 in the HDAC1 inhibitor group compared with the control group, the expression of CD86 in the combination group was significantly higher than that in HDAC11 group. Our results provide preliminary evidence that HDACs may be involved in regulating anti-tumor immune response through AA-mediated macrophage polarization (Fig. 6G).

## Discussion

HDAC1 and HDAC11 are closely related to the development of HCC. The expression of the retinoblastoma-interacting zinc finger (RIZ1) gene in HCC, affected by HDAC1-mediated acetylation of histone H3 lysine 9 (H3K9), was significantly lower than that in normal liver tissues [29]. The decreased acetylation level of H3K9 is also accompanied by

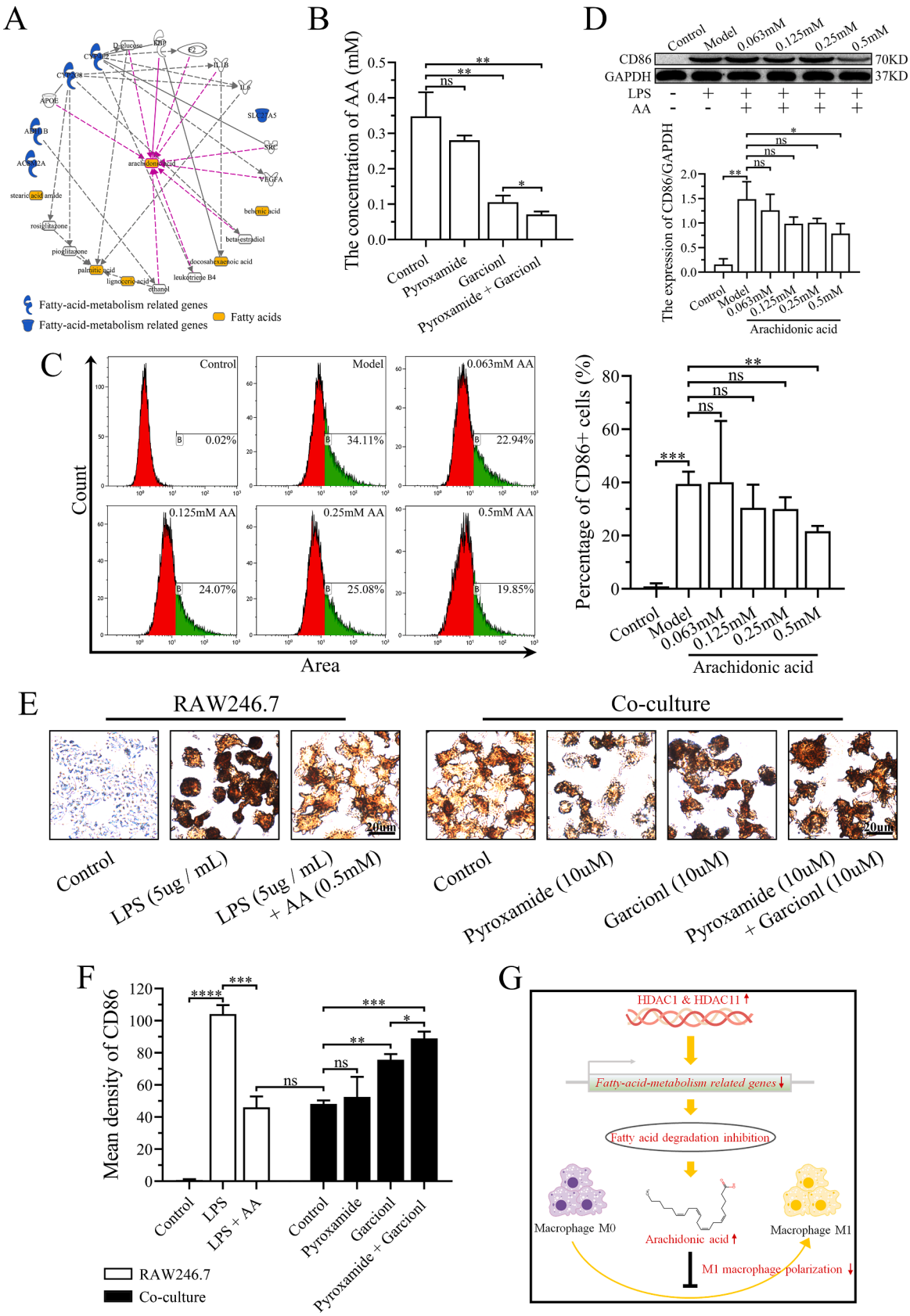


**Fig. 6.** HDACs may inhibit arachidonic acid (AA) metabolism and the polarization of M1 macrophages by down-regulating the expression of fatty-acid-metabolism related genes. **A.** Network of fatty-acid-metabolism related genes and fat acids constructed by IPA. **B.** Histogram of mean concentration of AA ($n = 3$). **C.** The expression of CD86 detected by flow cytometry ($n = 3$). **D.** The expression of CD86 detected by WB ($n = 3$). **E. The expression of CD86 detected by IHC (n = 3). F.** Histogram of mean density of CD86 **detected by IHC** ($n = 3$). **G.** Schematic: HDAC1 and HDAC11 can regulate AA metabolism in HCC cells, which is related to the polarization of macrophages in the tumor microenvironment. *: $p < 0.05$, **: $p < 0.01$, ***: $p < 0.001$, ****: $p < 0.0001$.

overexpression of HDAC11, promoting HCC by affecting the transcription of LKB1 [9]. Both HDAC1 and HDAC11 could form complexes with a variety of proteins, suggesting that they might have similar biological functions [30]. Consistently, the multivariate Cox regression model comprising HDAC1 and HDAC11 was demonstrated to **have a good predictive performance**, implying a potential synergistic role of these two HDACs in the development of HCC.

Macrophages, mast cells and Tregs may be important approaches by which HDACs exert immunosuppressive effects. It has been reported that HDAC1 and HDAC11 can inhibit the expression of IFN-γ [16,24]. Non-activated macrophages would polarize to M1 macrophages when they were exposed to IFN-γ [31]. Similarly, our data showed that high expression of HDAC1 and HDAC11 resulted in aggregation of macrophages M0 and deficiency of macrophages M1. Increased levels of activated mast cells were associated with a good prognosis in HCC patients [21], which was in line with our observations in GSE109211 dataset. However, a research on gastric cancer has shown that inactivated mast cells can inhibit the accumulation of macrophages M0, thereby reducing the proliferation and angiogenesis of tumor cells [32]. The role of mast cells in tumor immunity may be context-dependent, but there is no doubt that further research on the role of mast cells in the tumor microenvironment might help to understand the carcinogenic mechanism of HDACs. Furthermore, HDAC1 and HDAC11 could promote the production of Tregs [33,34], which may be due to the accumulation of fatty acids in the tumor microenvironment [35]. In conclusion, our results are consistent with previous reports that HDAC1 and HDAC11 may be able to influence the microenvironment.

HDACs can participate in metabolic reprogramming by inhibiting fatty acid degradation [36]. Increased level of fatty acids, regulated by mammalian target of rapamycin (mTOR), could promote the development of HCC [37]. HDAC inhibitors could significantly down regulate the phosphorylation level of Akt, which was the upstream protein of mTOR [38]. Therefore, PI3K / Akt / mTOR activation might be a potential mechanism for HDACs to increase fatty acid levels. The accumulation of fatty acids led to the loss of $CD4^+$ T cells and $CD8^+$ T cells functions, which might be related to its oxidative damage to mitochondria [26]. In addition, by participating in palmitoylation of transducer and activator of transcription 3 (STAT3), fatty acids have been shown to promote the activation of STAT3 signaling pathway before tumorigenesis [35]. Conditional knockout of STAT3 in hematopoietic cells caused the decrease of IL-23 secretion in tumor-associated macrophages, which inhibited the activation of Tregs and reduced the expression of IL-10 [39]. STAT3 played an important role in inflammation and immune response. It could not only induce inflammation to promote tumorigenesis, but also activate Tregs to weaken anti-tumor immunity [39]. This special mechanism may explain the reason why the accumulation of fatty acids is always conducive to the occurrence and development of HCC, suggesting that **the level of** of fatty acids is related to the microenvironment.

Our results showed that ACSM2A, ADH1B, CYP2C8, CYP4F2 and SLC27A5 are downstream targets of HDACs. ACSM2A and ADH1B play an important part in fatty acid oxidation and lipid synthesis respectively [40,41]. Both CYP4F2 and CYP2C8 are cytochrome P450, which have been widely reported as key enzymes of arachidonic acid (AA) [42,43]. Studies have shown that AA present at **certain** high concentrations in the tumor microenvironment [44] and can inhibit the polarization of macrophages M1 [45], suggesting that the HDACs-mediated decreased expression of CYP2C8 and CYP4F2 may inhibit anti-tumor immunity by affecting macrophage activation (Fig. 6G). Little is known about the role of these fatty-acid-metabolism related genes in HCC, especially, in tumor immunity. However, it is undeniable that in-depth study of these genes may help to further understand the changes in anti-tumor immunity mediated by fatty-acid-metabolism in HCC.

In summary, we found that HDAC1 and HDAC11 might play a synergistic immunosuppressive role in HCC progression. Down regulated fatty-acid-metabolism related genes modulated by HDACs might contribute to the obstacle of macrophage M1 polarization, which needs to be validated in our future *in vivo* and *in vitro* studies with specific knockout cell lines and animal models.

## Conclusion

In conclusion, high expression of HDAC1 and HDAC11 together lead to poor prognosis of HCC patients. They may play an important role in the inhibition of macrophages M1 polarization by regulating fatty-acid-metabolism related genes (ACSM2A. ADH1B, CYP2C8, CYP4F2 and SLC27A5). Our results suggest that HDACs-metabolism-immunity axis is a potential immunotherapeutic pathway for HCC, which provides a new insight for future research.

## Availability of data and materials

The datasets used or analyzed during the current study are available from the corresponding author on reasonable request.

## Funding

This work was supported by grants from National Natural Sciences Foundation of China (81873219, 81774180), Natural Science Foundation of Jiangsu Province (BK20181425), and Young Elite Scientists Sponsorship Program by CACM (CACM-2018-QNRC2-B07). In addition, this work was also financially supported in part by the grants from a project funded by the Priority Academic Program Development of Jiangsu Higher Education Institutions (PAPD) and Postgraduate Research & Practice Innovation Program of Jiangsu Province (KYCX22_1884).

## CRediT authorship contribution statement

**Lei Bi:** - Conceptualization, - Methodology, - Investigation, - Funding acquisition, - review & editing. **Linxin Teng:** - Writing - original draft, -Software. **Zhengjun Li:** - Writing, - Data curation, - Visualization, - Validation. **Yipeng Shi:** - Formal analysis, - Software. **Zihan Gao:** - Data curation, - Validation. **Yang Yang:** -Visualization, - Validation. **Yunshan Wang:** - Conceptualization, - Supervision, - review & editing.

## Declaration of Interest Statement

The authors declare that there are no conflicts of interest.

## Acknowledgments

We would like to thank experiment center for science and technology of Nanjing University of Chinese Medicine for providing us with experimental instruments.

## Supplementary materials

Supplementary material associated with this article can be found, in the online version, at doi:10.1016/j.tranon.2022.101547.

## References

[1] E Seto, M. Yoshida, Erasers of histone acetylation: the histone deacetylase enzymes, Cold Spring Harb. Perspect. Biol. 6 (2014), a018713, https://doi.org/10.1101/cshperspect.a018713.
[2] L Gao, MA Cueto, F Asselbergs, P. Atadja, Cloning and functional characterization of HDAC11, a novel member of the human histone deacetylase family, J. Biol. Chem. 277 (2002) 25748–25755, https://doi.org/10.1074/jbc.M111871200.
[3] TCS Ho, AHY Chan, A. Ganesan, Thirty Years of HDAC Inhibitors: 2020 Insight and Hindsight, J. Med. Chem. 63 (2020) 12460–12484, https://doi.org/10.1021/acs.jmedchem.0c00830.

[4] H Ji, Y Zhou, X Zhuang, Y Zhu, Z Wu, Y Lu, et al., HDAC3 deficiency promotes liver cancer through a defect in H3K9ac/H3K9me3 transition, Cancer Res. 79 (2019) 3676–3688, https://doi.org/10.1158/0008-5472.CAN-18-3767.
[5] B He, L Dai, X Zhang, D Chen, J Wu, X Feng, et al., The HDAC inhibitor quisinostat (JNJ-26481585) supresses hepatocellular carcinoma alone and synergistically in combination with sorafenib by G0/G1 phase arrest and apoptosis induction, Int. J. Biol. Sci. 14 (2018) 1845–1858, https://doi.org/10.7150/ijbs.27661.
[6] K Freese, T Seitz, P Dietrich, SML Lee, WE Thasler, A Bosserhoff, et al., Histone deacetylase expressions in hepatocellular carcinoma and functional effects of histone deacetylase inhibitors on liver cancer cells in vitro, Cancers 11 (2019) 1587, https://doi.org/10.3390/cancers11101587.
[7] KJ Falkenberg, RW. Johnstone, Histone deacetylases and their inhibitors in cancer, neurological diseases and immune disorders, Nat. Rev. Drug Discov. 13 (2014) 673–691, https://doi.org/10.1038/nrd4360.
[8] DF Tough, PP Tak, A Tarakhovsky, RK Prinjha, Epigenetic drug discovery: breaking through the immune barrier, Nat. Rev. Drug Discov. 15 (2016) 835–853, https://doi.org/10.1038/nrd.2016.185.
[9] L Bi, Y Ren, M Feng, P Meng, Q Wang, W Chen, et al., HDAC11 regulates glycolysis through the LKB1/AMPK signaling pathway to maintain hepatocellular carcinoma stemness, Cancer Res. 81 (2021) 2015–2028, https://doi.org/10.1158/0008-5472.CAN-20-3044.
[10] Y-H Lee, D Seo, K-J Choi, JB Andersen, M-A Won, M Kitade, et al., Antitumor effects in hepatocarcinoma of isoform-selective inhibition of HDAC2, Cancer Res. 74 (2014) 4752–4761, https://doi.org/10.1158/0008-5472.CAN-13-3531.
[11] TB Toh, JJ Lim, EK-H Chow, Epigenetics of hepatocellular carcinoma, Clin. Transl. Med. 8 (2019) 13, https://doi.org/10.1186/s40169-019-0230-0.
[12] Q Yang, J Wei, L Zhong, M Shi, P Zhou, S Zuo, et al., Cross talk between histone deacetylase 4 and STAT6 in the transcriptional regulation of arginase 1 during mouse dendritic cell differentiation, Mol. Cell. Biol. 35 (2015) 63–75, https://doi.org/10.1128/MCB.00805-14.
[13] C Govindaraj, P Tan, P Walker, A Wei, A Spencer, M. Plebanski, Reducing TNF receptor 2+ regulatory T cells via the combined action of azacitidine and the HDAC inhibitor, panobinostat for clinical benefit in acute myeloid leukemia patients, Clin. Cancer Res. 20 (2014) 724–735, https://doi.org/10.1158/1078-0432.CCR-13-1576.
[14] R Tao, EF de Zoeten, E Ozkaynak, C Chen, L Wang, PM Porrett, et al., Deacetylase inhibition promotes the generation and function of regulatory T cells, Nat. Med. 13 (2007) 1299–1307, https://doi.org/10.1038/nm1652. Epub 2007 Oct 7.
[15] EF de Zoeten, L Wang, H Sai, WH Dillmann, WW. Hancock, Inhibition of HDAC9 increases T regulatory cell function and prevents colitis in mice, Gastroenterology 138 (2010) 583–594, https://doi.org/10.1053/j.gastro.2009.10.037.
[16] DM Woods, KV Woan, F Cheng, AL Sodré, D Wang, Y Wu, et al., T cells lacking HDAC11 have increased effector functions and mediate enhanced alloreactivity in a murine model, Blood 130 (2017) 146–155, https://doi.org/10.1182/blood-2016-08-731505.
[17] JL Guerriero, A Sotayo, HE Ponichtera, JA Castrillon, AL Pourzia, S Schad, et al., Class IIa HDAC inhibition reduces breast tumours and metastases through anti-tumour macrophages, Nature 543 (2017) 428–432, https://doi.org/10.1038/nature21409.
[18] K Qu, LC Zaba, AT Satpathy, PG Giresi, R Li, Y Jin, et al., Chromatin accessibility landscape of cutaneous T Cell lymphoma and dynamic response to HDAC inhibitors, Cancer Cell 32 (2017) 27–41, https://doi.org/10.1016/j.ccell.2017.05.008.
[19] DO Adeegbe, Y Liu, PH Lizotte, Y Kamihara, AR Aref, C Almonte, et al., Synergistic immunostimulatory effects and therapeutic benefit of combined histone deacetylase and bromodomain inhibition in non-small cell lung cancer, Cancer Discov. 7 (2017) 852–867, https://doi.org/10.1158/2159-8290.CD-16-1020.
[20] S Roessler, H-L Jia, A Budhu, M Forgues, Q-H Ye, J-S Lee, et al., A unique metastasis gene signature enables prediction of tumor relapse in early-stage hepatocellular carcinoma patients, Cancer Res. 70 (2010) 10202–10212, https://doi.org/10.1158/0008-5472.CAN-10-2607.
[21] R Pinyol, R Montal, L Bassaganyas, D Sia, T Takayama, G-Y Chau, et al., Molecular predictors of prevention of recurrence in HCC with sorafenib as adjuvant treatment and prognostic factors in the phase 3 STORM trial, Gut 68 (2019) 1065–1075, https://doi.org/10.1136/gutjnl-2018-316408.
[22] LM Butler, Y Webb, DB Agus, B Higgins, TR Tolentino, MC Kutko, et al., Inhibition of transformed cell growth and induction of cellular differentiation by pyroxamide, an inhibitor of histone deacetylase, Clin. Cancer Res. 7 (2001) 962–970, https://doi.org/10.1002/anie.201207405.
[23] SI Son, D Su, TT Ho, H Lin, Garcinol Is an HDAC11 Inhibitor, ACS Chem. Biol. 15 (2020) 2866–2871, https://doi.org/10.1021/acschembio.0c00719.
[24] R Deng, P Zhang, W Liu, X Zeng, X Ma, L Shi, et al., HDAC is indispensable for IFN-γ-induced B7-H1 expression in gastric cancer, Clin. Epigen. 10 (2018) 153, https://doi.org/10.1186/s13148-018-0589-6.
[25] EH Ma, G Bantug, T Griss, S Condotta, RM Johnson, B Samborska, et al., Serine is an essential metabolite for effector T Cell expansion, Cell Metab. 25 (2017) 345–357, https://doi.org/10.1016/j.cmet.2016.12.011.
[26] C Ma, AH Kesarwala, T Eggert, J Medina-Echeverz, DE Kleiner, P Jin, et al., NAFLD causes selective CD4(+) T lymphocyte loss and promotes hepatocarcinogenesis, Nature 531 (2016) 253–257, https://doi.org/10.1038/nature16969.
[27] S Hua, F Chen, G Xu, S. Gou, Multifunctional platinum(IV) complexes as immunostimulatory agents to promote cancer immunochemotherapy by inhibiting tryptophan-2,3-dioxygenase, Eur. J. Med. Chem. 169 (2019) 29–41, https://doi.org/10.1016/j.ejmech.2019.02.063.
[28] Z Li, H Li, Z-B Zhao, W Zhu, P-P Feng, X-W Zhu, et al., SIRT4 silencing in tumor-associated macrophages promotes HCC development via PPARδ signalling-mediated alternative activation of macrophages, J. Exp. Clin. Cancer Res. 38 (2019) 469, https://doi.org/10.1186/s13046-019-1456-9.
[29] C Zhang, H Li, Y Wang, W Liu, Q Zhang, T Zhang, et al., Epigenetic inactivation of the tumor suppressor gene RIZ1 in hepatocellular carcinoma involves both DNA methylation and histone modifications, J. Hepatol. 53 (2010) 889–895, https://doi.org/10.1016/j.jhep.2010.05.012.
[30] P Joshi, TM Greco, AJ Guise, Y Luo, F Yu, AI Nesvizhskii, et al., The functional interactome landscape of the human histone deacetylase family, Mol. Syst. Biol. 9 (2013) 672, https://doi.org/10.1038/msb.2013.26.
[31] S Huang, W Hendriks, A Althage, S Hemmi, H Bluethmann, R Kamijo, et al., Immune response in mice that lack the interferon-gamma receptor, Science 259 (1993) 1742–1745, https://doi.org/10.1126/science.8456301.
[32] MF Eissmann, C Dijkstra, A Jarnicki, T Phesse, J Brunnberg, AR Poh, et al., IL-33-mediated mast cell activation promotes gastric cancer through macrophage mobilization, Nat. Commun. 10 (2019) 2735, https://doi.org/10.1038/s41467-019-10676-1.
[33] M Xia, J Liu, S Liu, K Chen, H Lin, M Jiang, et al., Ash1l and lnc-Smad3 coordinate Smad3 locus accessibility to modulate iTreg polarization and T cell autoimmunity, Nat. Commun. 8 (2017) 15818, https://doi.org/10.1038/ncomms15818.
[34] D Buglio, NM Khaskhely, KS Voo, H Martinez-Valdez, Y-J Liu, A. Younes, HDAC11 plays an essential role in regulating OX40 ligand expression in Hodgkin lymphoma, Blood 117 (2011) 2910–2917, https://doi.org/10.1182/blood-2010-08-303701.
[35] J Niu, Y Sun, B Chen, B Zheng, GK Jarugumilli, SR Walker, et al., Fatty acids and cancer-amplified ZDHHC19 promote STAT3 activation through S-palmitoylation, Nature 573 (2019) 139–143, https://doi.org/10.1038/s41586-019-1511-x.
[36] E Hurtado, Y Núñez-Álvarez, M Muñoz, C Gutiérrez-Caballero, J Casas, AM Pendás, et al., HDAC11 is a novel regulator of fatty acid oxidative metabolism in skeletal muscle, FEBS J. 288 (2021) 902–919, https://doi.org/10.1111/febs.15456.
[37] J Li, Q Huang, X Long, J Zhang, X Huang, J Aa, et al., CD147 reprograms fatty acid metabolism in hepatocellular carcinoma cells through Akt/mTOR/SREBP1c and P38/PPARα pathways, J. Hepatol. 63 (2015) 1378–1389, https://doi.org/10.1016/j.jhep.2015.07.039.
[38] HMW Verheul, B Salumbides, K Van Erp, H Hammers, DZ Qian, T Sanni, et al., Combination strategy targeting the hypoxia inducible factor-1 alpha with mammalian target of rapamycin and histone deacetylase inhibitors, Clin. Cancer Res. 14 (2008) 3589–3597, https://doi.org/10.1158/1078-0432.CCR-07-4306.
[39] M Kortylewski, H Xin, M Kujawski, H Lee, Y Liu, T Harris, et al., Regulation of the IL-23 and IL-12 balance by Stat3 signaling in the tumor microenvironment, Cancer Cell 15 (2009) 114–123, https://doi.org/10.1016/j.ccr.2008.12.018.
[40] LD Morales, DT Cromack, D Tripathy, M Fourcaudot, S Kumar, JE Curran, et al., Further evidence supporting a potential role for ADH1B in obesity, Sci. Rep. 11 (2021) 1932, https://doi.org/10.1038/s41598-020-80563-z.
[41] R. van der Sluis, Analyses of the genetic diversity and protein expression variation of the acyl: CoA medium-chain ligases, ACSM2A and ACSM2B, Mol. Genet. Genom. 293 (2018) 1279–1292, https://doi.org/10.1007/s00438-018-1460-3.
[42] W-Y Kim, S-J Lee, J Min, K-S Oh, D-H Kim, H-S Kim, et al., Identification of novel CYP4F2 genetic variants exhibiting decreased catalytic activity in the conversion of arachidonic acid to 20-hydroxyeicosatetraenoic acid (20-HETE), Prostaglandins Leukot. Essent. Fatty Acids 131 (2018) 6–13, https://doi.org/10.1016/j.plefa.2018.02.003.
[43] R Lee, V Kim, Y Chun, D Kim, Structure-functional analysis of human cytochrome P450 2C8 using directed evolution, Pharmaceutics 13 (2021) 1429, https://doi.org/10.3390/pharmaceutics13091429.
[44] R Dietze, MK Hammoud, M Gómez-Serrano, A Unger, T Bieringer, F Finkernagel, et al., Phosphoproteomics identify arachidonic-acid-regulated signal transduction pathways modulating macrophage functions with implications for ovarian cancer, Theranostics 11 (2021) 1377–1395, https://doi.org/10.7150/thno.52442.
[45] Y Cheng, Y Feng, Z Xia, X Li, J Rong, ω-Alkynyl arachidonic acid promotes anti-inflammatory macrophage M2 polarization against acute myocardial infarction via regulating the cross-talk between PKM2, HIF-1α and iNOS, Biochim. Biophys. Acta 1862 (2017) 1595–1605, https://doi.org/10.1016/j.bbalip.2017.09.009.